THE
PHYSICAL REVIEW

A journal of experimental and theoretical physics established by E. L. Nichols in 1893

SECOND SERIES, VOL. 78, NO. 6 JUNE 15, 1950

Beta-Spectra of Gaseous A^{41} and O^{15} *

HAROLD BROWN AND VICTOR PEREZ-MENDEZ
Pupin Physics Laboratories, Columbia University, New York, New York

(Received November 21, 1949)

A magnetic semicircular focusing spectrometer with a radius of curvature of 13.6 cm has been constructed and adapted for the measurement of the β-ray spectra of emitters in gaseous phase.

The radioactive gases were produced by deuteron bombardment of gaseous samples in a cyclotron using special probes.

A^{41} (109 min.) produced by the $A^{40}(d, p)$ reaction showed a spectrum of maximum energy (1.245±0.005) Mev and an allowed spectrum shape down to at least 200 kev.

The half-life of O^{15}, produced by the $N^{14}(d, n)$ reaction, was determined to be (118.0±0.6) sec. The end point of its positrons was (1.638±0.005) Mev. The Fermi plot departed from linearity at 300 kev, but this effect may be of experimental origin.

I. INTRODUCTION

OVER a period of fifteen years a vast quantity of experimental data concerning β-ray spectra has been accumulated, most of it misleading in greater or lesser degree. In recent months, however, the use of very thin sources[1–3] has tended to put the Fermi theory of allowed transitions[4–7] on firmer ground than previously, and the discovery and analysis of spectra of various forbidden shapes[8–10] has given strong confirmation of the Gamow-Teller[5] modification as regards forbidden transitions. However, several discrepancies have still to be clarified.

Two classes of emitters have not hitherto been thoroughly investigated. These are (a) rare gas emitters and (b) short-lived activities (a few minutes or less). The two categories overlap to some extent. The former includes such isotopes as A^{41}, Ne^{23}, and He^{6}; the latter includes most of the well-known Wigner series of "super-allowed transitions," those in which the nuclear wave functions are so alike before and after the transition that the matrix element involved is nearly equal to unity. Most of the "mirror image" nuclei are the emitters and products of this series.

The experiments described here measure the half-lives and β-spectra of two examples from these groups from about 250 kev to 4.5 Mev with gaseous sources. In the case of the short-lived emitters, use of a gas facilitates a rapid change of the source, and by monitoring the activity of the flow the necessity of accounting for the decay of the source is removed. The window necessary to keep the gas in the source chamber distorts the spectra below 250 kev. However, by confining the investigation to spectra of end-point energy greater than 1 Mev, not only can the end points be obtained but a decision can be reached on whether the spectra are of the allowed shape or not ($\frac{3}{4}$ of the spectrum is sufficient for this purpose). Previously, short-lived β-spectra measurements using a β-spectrometer have included continuous β-spectra of N^{13} (10-min. half-life)[11] and line spectra of Al^{28} (3 min.).[12] An entirely different method, involving the bombardment of sources already in the spectrometer, was recently used by Hornyak *et al.*,[13] to measure the very high energy

* Supported in part by the AEC.

[1] R. D. Albert and C. S. Wu, Phys. Rev. **74**, 847 (1948).
[2] C. S. Wu and R. D. Albert, Phys. Rev. **75**, 315 (1949).
[3] L. Feldman and C. S. Wu, Phys. Rev. **76**, 697 (1949).
[4] E. Fermi, Zeits. f. Physik **88**, 161 (1934).
[5] G. Gamow and E. Teller, Phys. Rev. **49**, 895 (1936).
[6] E. J. Konopinski and G. E. Uhlenbeck, Phys. Rev. **60**, 308 (1941).
[7] E. P. Wigner, Phys. Rev. **56**, 519 (1939).
[8] Slack, Braden, and Shull, Phys. Rev. **75**, 1965 (1949).
[9] L. M. Langer and H. C. Price Jr., Phys. Rev. **76**, 641 (1949).
[10] C. S. Wu and L. Feldman, Phys. Rev. **76**, 693, 696, 698 (1949).
[11] Cook, Langer, Price, and Sampson, Phys. Rev. **74**, 502 (1948).
[12] Benes, Hedgran, and Hole, Arkiv. f. Mat. Astro. Fys. **35a**, No. 12 (1948).
[13] Hornyak, Dougherty, and Lauritsen, Phys. Rev. **74**, 1727 (1948).

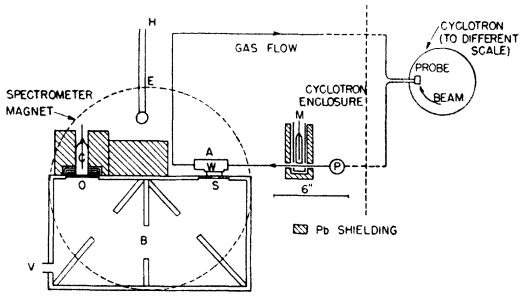

FIG. 1. Schematic diagram of the spectrometer and the pumping system for radioactive gases. A is the source chamber and W the thin cellophane window. S is the entrance slit, O the exit slit, and B the central defining baffle. V is the exhaust outlet and C the spectrometer counter, H the shaft and E the rotating coil of the spinner. M is the monitor counter, and P the circulating pump.

spectra (about 12 Mev) of the very short-lived activities of B^{12} (0.022 sec.) and Li^8 (0.8 sec.). Cloud-chamber measurements of short-lived spectra were made over ten years ago[14] but were subject to large scattering errors.

II. APPARATUS

The spectrometer was of the 180° semicircular focusing type patterned after the design of Lawson and Tyler.[15,16] The magnetic field was obtained by using an electromagnet of 4-in. core diameter to which pole tips 16 in. in diameter and 1 in. thick were attached. The maximum obtainable field in the useful region was 1500 gauss, constant to about 0.1 percent. Current was supplied by a voltage stabilized generator which was constant to better than $\frac{1}{2}$ percent. The measurement of the magnetic field was obtained by balancing the rectified a.c. signal generated in a rotating coil in the magnetic field against a standard voltage. The field is inversely proportional to R_s, the resistance on a voltage divider. Measurements showed that the change in magnetic field never exceeded 0.2 percent in 20 minutes.

The vacuum envelope for the spectrometer, a rectangular parallelepiped 2 in.×8 in.×16 in., (Fig. 1) is of brass with aluminum cover plates. The brass surfaces are everywhere covered by polystyrene strips $\frac{1}{4}$ in. thick. These are designed to reduce the scattering, as the backscattering coefficients† are roughly Cu≃0.30, Al≃0.10, polystyrene≃0.03. The spectrometer chamber was machined near the source fitting (S) so as to increase the distance from the (polystyrene-lined) brass of the spectrometer wall to the source position which can be taken either as the solid source, where used, or the first slit (which acts as a virtual source in the case of gaseous emitters).

Two sets of baffles are employed in this spectrometer; one limits the beam height to $\frac{3}{4}$ in. and the other limits the angular spread. The baffle plates are constructed in sandwich form. The side facing the beam is made of $\frac{1}{4}$-in. polystyrene, to reduce scattering; the other side is made of $\frac{1}{8}$-in. brass, which is sufficient to stop 4.5-Mev betas. The edges of both halves were beveled to the most advantageous angles. The exit and entrance slits are 2.0 cm high and either 0.5 or 1.0 cm wide. For spectra whose end points are less than 2 Mev, a 0.15-cm thickness of brass is used for entrance and exit slits; for those greater than 2 Mev, a 0.30-cm thickness is used.

The pressure in the spectrometer is always less than 1μ of Hg which is equivalent to a weight per unit area (over a 45-cm electron path length) of 0.06μ g/cm².

The counters used were of the thin end-window type, using mica windows of thickness 1.4 mg/cm². Corrections for variation in counting efficiency with electron energy, and for counting losses due to deadtime, were negligible.

The correction for absorption and scattering in the counter window was made by finding the numbers of electrons of various energies (from a P^{32} source) counted with various thicknesses of mica interposed before the counter window. Using the relation $N=N_0e^{-kw}$ for the number of electrons transmitted, the correction curve shown in Fig. 2 was obtained.

III. THE SOURCE CHAMBER

The novel feature of this spectrometer is the incorporation of a source chamber which allows the spectrum of the activity to be investigated when the substance is in the gaseous phase.

A. Construction

The source chamber, shown in Fig. 3, consists of a 0.5-mm sheet of aluminum welded to a $\frac{1}{8}$-in. aluminum top and semicircular sides. A thin window is attached by rubber gaskets and the tube is sealed into the spectrometer by the usual gasket-compression arrangement.

Brass tubing is attached to the sides of the chamber for the purpose of introducing the gas. The monitor (Section IV) is attached to the system along the line through which the gas flows into the source chamber.

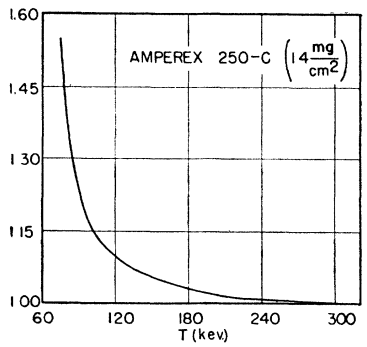

FIG. 2. Window transmission correction for the counter used.

[14] Fowler, Delsasso, and Lauritsen, Phys. Rev. **49**, 561 (1936).
[15] J. L. Lawson and A. W. Tyler, Rev. Sci. Inst. **11**, 6 (1940).
[16] A. K. Saha, Ind. J. Phys. **19**, 97 (1945).
† These are rough values obtained from measurements in this laboratory for saturation back-scattering.

B. Instrumental Scattering

The reliability of the results obtained is limited by the scattering of β-particles which may take place either in the source chamber or in the spectrometer.

From geometrical consideration of Fig. 3a, b it can be seen that we may neglect the single scattering into the effective beam from all surfaces except a narrow section of the aluminum backing, the edges of the entrance slit, and the thin window which isolates the radioactive gas. Since the scattering coefficient of all surfaces involved is 10 percent or less, double scattering can be neglected as a source of error in the spectrum.

The scattering from the thin aluminum backing has been estimated[17] from the solid angles involved and the reflection coefficient, which has an upper limit of 0.2 at 200 kev.[18] The ratio of the number back-scattered and passing through the slit to those passing through without scattering is approximately 0.2 percent (calculated on the basis of straight line trajectories) for a typical point P in the middle of the source volume which contribute to the beam. For those electrons emitted very near the backing a larger fraction of those entering the beam will have been scattered into it, but these form only a small fraction of the total emitted; those electrons emitted near the window will have virtually no chance of being reflected into the beam from the backing. The average ratio over the entire volume for such scattering is less than 1 percent.

The scattering from the first slit is similar to that of the other baffles; both scattering and partial penetration of electrons through the edges occur. Since this slit is the closest to the source, its effect will be the greatest.

Using an average distance of 3.0 cm from the source point to the slit, not more than 0.1–0.2 percent of the β-particles which emerge in the detectable beam should be scattered from the first slit. In view of the possibility of large small-angle scattering, however, this estimate was checked experimentally when the A^{41} spectrum was taken. In this case spectra were taken with both the 0.3 and 0.15-cm thickness slits, and found to agree down to about 200 kev, indicating that the first slit has a negligible effect on the spectra above 200 kev.

The distortion of the β-ray spectra by the window separating the source from the spectrometer is best evaluated with the aid of the data of White and Millington,[19] who found that a thin film in front of a monoenergetic beam of electrons produces an energy distribution whose maximum occurs near $T_0-\Delta T$, where T_0 is the initial energy and ΔT is some average energy loss (given by the range-energy curve), and, furthermore, that the breadth (full width at half-maximum) of the distribution is also of the order of ΔT, or $\Delta(H\rho)$ in momentum units. For sufficiently large values of ΔT the low energy tail of the distribution becomes extremely pronounced.

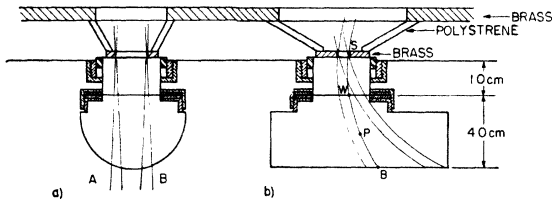

FIG. 3. (*a*) Detail drawing of source chamber, side section. *A* and *B* are the limiting β-ray trajectories which enter the spectrometer counter without scattering. (*b*) Detail drawing of source chamber, front section. The limiting detectable trajectories are shown. Point *B* is a point on the backing, *P* is a source point, W a point on the window, and *S* at the slit.

To determine the effect of the thin window on the source chamber, the ratio $\Delta(H\rho)/H\rho$, as well as the average energy loss ΔT, has been calculated as a function of the electron energy. Table I gives the quantities involved, with ΔT and $\Delta(H\rho)/H\rho$ calculated for a window 2.5 mg/cm^2.

The two effects (shift and spread of energies) can be estimated from this table. The shift at very high energies is nearly constant, and must be considered in evaluating the end point from the observed spectra. With decreasing energy the shift increases; the important quantity is this increase, which tends to distort the spectrum. Actually one should add to the measured energy obtained from the reading on the spinner the value ΔT before plotting the curves. This correction, however, would be negligible above about 200 kev (for 2.5 mg/cm^2 window); so the procedure followed has been to plot the data as obtained, and subsequently to add ΔT at high energy to get the end point. It is also in the region of about 250 kev that the straggling becomes comparable with the resolution width. One would then expect that the large area under the low energy tail would cause a rise in the observed number of the β-rays at those energies. Above the 250-kev region the window effects can therefore be neglected.

C. Resolution and Intensity

Graphical determinations have been made of the solid angle subtended by the entire slit system (including the entrance slit) at various points in the source volume, as a function of the radius of curvature. For 1.0-cm entrance and exit slits, the results are shown (Fig. 4) for two points. Curve *A* represents $T(\rho)$ for a source point 2.0 cm below and 0.2 cm to the right of the center of the exit slit (this corresponding to a point near the top of the source); curve *B* represents that for a source point 6.0 cm below and 0.5 cm to the right (near the backing). These and many other such curves show that the expected mean radius of curvature is 13.5 to 13.6 cm; that a point in the source near the slit has $T_{max}\simeq 0.25$ percent (for 1.0-cm slit); a distant one

[17] Bethe, Rose, and Smith, Proc. Am. Phil. Soc. **78**, 573 (1938).
[18] Rutherford, Chadwick, and Ellis, *Radiations from Radioactive Substances*, (Cambridge University Press, London, 1930) pp. 411–444.
[19] P. White and G. Millington, Proc. Roy. Soc. **A120**, 701 (1928).

TABLE I. Energy loss and straggling of electrons.

T(Mev)	4.0	0.8	0.4	0.3	0.25	0.20	0.15
ΔT(kev)	4.5	4.5	7.0	8.5	9.0	10.0	11.0
$\Delta(H\rho)/H\rho$ in %	0.1	0.4	1.0	1.3	1.7	2.9	4.2

has $T_{max}\simeq 0.16$ percent. These correspond to angles in the median plane of about 30° and 18°. For 0.5-cm slits these angles (and transmissions) are divided by about 2. The resolutions observed on the transmission curves are 3.5 to 4.0 percent for wide (1.0 cm) and about one-half of that for the narrow (0.5 cm) slits. Since the transmission curves corresponding to various points in the source are displaced relative to each other, over-all figures for the resolutions might be put at 5.0 and 2.5 percent respectively.

The relative transmissions for the solid and gaseous cases can be obtained from Fig. 3b. If the difference in length of the curved paths passing through different points of the slit is neglected, the effective volume contributing to the electron beam passing through an element dS of area on the slit is approximately LdS where L is this length.

The important thing to notice about the beam from the gaseous source emerging from the entrance slit is that it has the same angular distribution as the beam from the solid source actually entering the chamber. Since the emergent beams over the useful solid angle are the same in intensity distribution for the two cases, the approximate intensity and resolution for the gaseous sources can be ascertained by employing solid sources instead.

To summarize the conclusions drawn, we have for a gaseous source using 0.5-cm slits:

$T_m\simeq 0.001$, $\delta\simeq 0.02$ and the active volume $2.0\times 4\times 0.5=4$ cm³.

With 1.0-cm slits, $T_m\simeq 0.002$, $\delta\simeq 0.04$ and $V_a\simeq 8$ cm³.

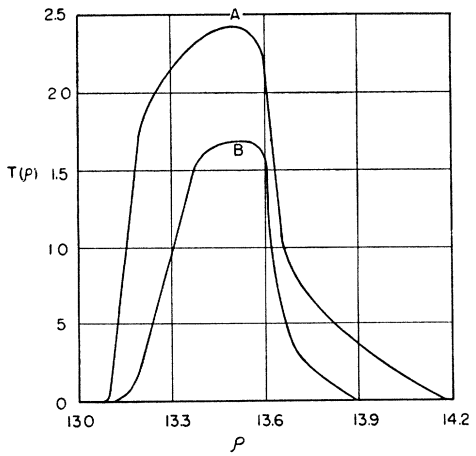

FIG. 4. Transmission curves determined graphically for two points in the source chamber. $T(\rho)$ is the fraction of the total solid angle subtended by the exit slit at the source point. ρ is the radius of the curvature (in cm) of the β-ray trajectory.

The average counting rate over a spectrum is given (for an approximately triangular resolution curve) by $nT_m\delta V_a$, where n is the number of disintegrations per second per cm³ in the "active volume" of the source.

IV. THE MONITOR AND GAS PROBE

To take account of the decay of the source and its variation in intensity as the bombarding cyclotron beam varies, an end-window geiger counter (Fig. 1) was placed along the gas pumping line about 8 cm from the source chamber. To avoid having the particles from the gas line travel in curved paths before being counted by the monitor counter, the entire system is magnetically shielded. Since positrons originating in the source chamber could travel in curved paths and produce γ-rays which might be counted by the monitor, the magnetic shield is surrounded by a $\frac{7}{8}$-in. thick lead shield. Changing the magnetic field in the spectrometer has no effect on the counting rate of the monitor so long as the source strength remains the same, indicating that the shielding is successful in making the count of the monitor directly proportional to the source strength. Without the shielding the monitor count changes by as much as a factor of two as the magnetic field varies.

The gas probe[20] consists of a water-cooled solid copper head with holes for gas flow. The bombardment chamber is covered with a copper window 1 mil thick. Deuteron beams of average current up to about 25μ amp. were used; of this about 15μ amp. hits the window and passes through the length (about 5 cm) of the bombardment chamber.

The gas to be bombarded is pumped through and, along with the gaseous products of deuteron-induced reactions, out of the probe. The tube carrying it passes out of the cyclotron enclosure (through the shielding) past the monitor counter and enters the source chamber of the spectrometer. The flow rate is high enough (several hundred cm³/sec.) so that the concentration of radioactive gas is effectively the same near the monitor and in the source chamber. Figure 1 shows the pumping system used with the gas probe.

V. SOLID SOURCES

The instrument was calibrated with the photoelectrons from annihilation radiation. Figure 5 shows the curve of intensity *vs.* the spinner reading for a thick lead foil (50 mg/cm²). Using both thick and thin radiators,[21,22] the value obtained for $1/R_{s0}$ corresponding to the known $H\rho$ of 2615 gauss-cm (or energy of $mc^2-E_{Pb,K}=422.5$ kev) is 4.20×10^{-4} mho.

Thus $H\rho=2615\times(2380/R_s)$ gauss-cm so that we have a conversion formula to give the momentum in

[20] H. Brown and V. Perez-Mendez, Phys. Rev. **75**, 1286 (1949).
[21] Jensen, Laslett, and Pratt, Phys. Rev. **75**, 458 (1949).
[22] Hornyak, Lauritsen, and Rasmussen, Phys. Rev. **76**, 731 (1949).

gauss-cm corresponding to a given reading on the voltage divider at balance.

The radius of curvature obtained from the value of $H\rho$ for a given voltage divider setting (immediately above) and the magnetic field for that same setting (obtained from the comparison with the G. E. Fluxmeter) is $\rho = 13.62$ cm. This is quite close to the geometrically predicted value for the maximum of the $T(\rho)$ curve (about 13.6).

To check this calibration the internal conversion electrons from the 185-kev γ-ray[23,24] of In^{114} were investigated, and found to agree with the locations observed on the Columbia solenoidal spectrometer[25] (1465 and 1580 gauss-cm). The resolution, using a 0.5-cm wide solid source and a detector slit of equal width, was about 3 percent.

In order to check the over-all performance of the spectrometer, the spectrum[26] of P^{32} was measured, using a number of thin samples. The spectrum obtained gave a Fermi plot linear approximately down to 200 kev, with an end point at 3.39 mc^2. The agreement with the results of previous investigations leads us to conclude that this semicircular-focusing spectrometer gives reliable information on the number of β-rays of various energies emitted from the vicinity of the source.

VI. RESULTS

A. Argon 41

The first gas whose spectrum was investigated was A^{41}. It was produced in the gas probe by deuteron bombardment of spectroscopically pure argon (which is 99.6 percent A^{40}). The A^{41} is produced by a (d, p) reaction, the beam consisting of 15 to 25μ amps. of 8-Mev deuterons, and the bombardment was for 45 to 70 minutes in various cases. The probe was arranged so that the cyclotron beam fell on the window by attaching the probe to the pumping system and bombarding nitrogen, which produces a short-lived activity (2-min. O^{15}). The probe was then filled with argon and sealed off. Following the bombardment, the argon was transferred by expansion to an evacuated flask and from there to the previously evacuated source chamber which fits into the spectrometer. Because of the long half-life, continuous pumping is not necessary. The pressure of the argon in the source chamber was about 10 cm Hg so that its equivalent thickness is 0.8 mg/cm^2. The window thickness was 2.0 mg/cm^2.

In evaluating the data taken from the spectrometer and monitor counters, the background can be divided into two parts. The first is the (constant) part due to cosmic radiation, emission from the counter walls, etc. This is subtracted from the raw counting rates of both spectrometer and monitor counters to get the number of counts due to the activity under investigation. However, there is a second background which also must be subtracted. This fraction depends on the amount of activity in the source chamber; it consists of counts produced by γ-rays (of nuclear type and also from annihilation of positrons) or the photo-electrons and Compton electrons produced by them which register in the spectrometer counter. The counter was shielded from the direct γ-radiation by the lead shielding inside and outside the vacuum envelope, but the secondary electrons produced in various parts of the spectrometer, and particularly near the exit slit, have some probability of being detected. These portions are near the counter, so that the secondary electrons should not be too much affected by the magnetic field. Compton and photo-electrons produced in the exit slit which have enough energy to pass through the rest of the slit and register in the counter have a very small cross section for production. Calculation indicates, for instance, that if N positrons are incident on the entire slit, about $0.2\ N$ pass through the rectangular hole in it, and less than $0.005\ N$ Compton and photo-electrons produced by the annihilation of the positrons are counted—thus an additional fraction of $2\frac{1}{2}$ percent is introduced. This second background thus consists mainly of secondary electrons produced in the parts of the spectrometer near the exit slit, and of stray radiations from the sample under investigation.

Experiments have shown that in the energy region outside of the spectrum (for both directions of H) the ratio of this "background" to the monitor count is a constant. The same result is also obtained by covering the detector slit with the sliding gate. This ratio was

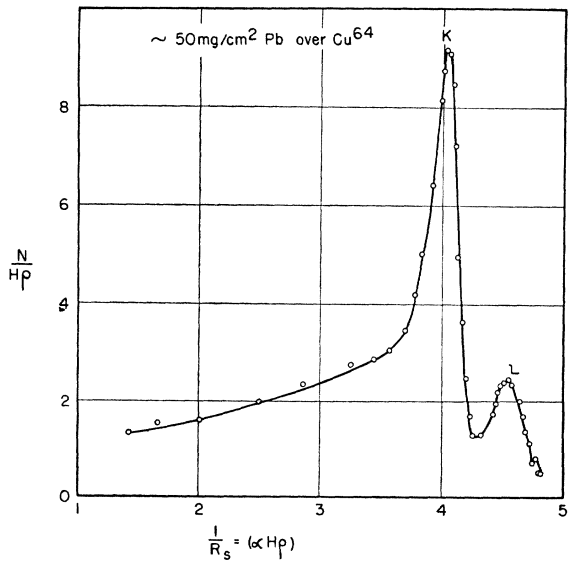

FIG. 5. Spectrum of the photo-electrons ejected from a thick lead radiator by the annihilation radiation of Cu^{64}. R_s is the reading on the potentiometer in ohms ($\times 10^4$). $1/R_s$ is proportional to the electron momentum. N is in arbitrary units, and $N/H\rho$ is the number of electrons per unit momentum range. Background has been subtracted.

[23] J. L. Lawson and J. M. Cork, Phys. Rev. **57**, 982 (1940).
[24] P. W. Levy, Plutonium Project Report, MonP-250, p. 26 (1947).
[25] Wu, Albert, and Feldman (private communication).
[26] K. Siegbahn, Phys. Rev. **70**, 127 (1946).

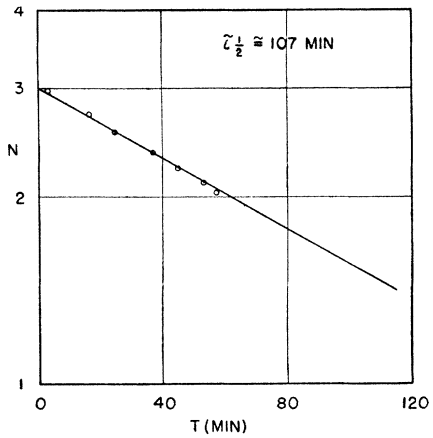

FIG. 6. Decay curve of A^{41}, taken simultaneously with the spectrum. N is in arbitrary units, T is the time in minutes. Only a few of the experimental points are shown.

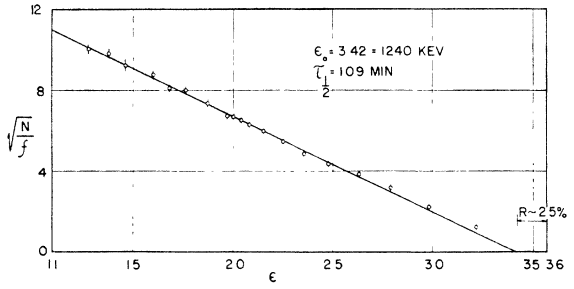

FIG. 7. Fermi plot of the A^{41} β-spectrum. ϵ is the electron energy (rest+kinetic) in units of mc^2. N is the number of electrons per unit momentum range, and f the Fermi function $\eta^2 F(Z, \epsilon)$. $(N/f)^{\frac{1}{2}}$ is in arbitrary units. The resolution is shown. Where the statistical error is greater than the size of the open circles, it is shown by the vertical lines.

therefore subtracted from the ratio of spectrometer counts to monitor counts in identical time intervals (following subtraction of the constant background) in order to obtain the true spectrum of the sample being investigated.

The spectrum of A^{41} was previously investigated in a cloud chamber by Kurie, Richardson, and Paxton.[27] They obtained, using the Konopinski-Uhlenbeck plot extrapolation, an end point of 1.5 Mev. Bleuler *et al.*,[28] using a coincidence-absorption method, concluded that the spectrum was complex, consisting of a 1.18-Mev negative electron group in cascade with a 1.3-Mev γ-ray 99.3 percent of the time, and a 2.55-Mev β-ray 0.7 percent of the time. They obtained a 109.4-min. half-life.

The decay curve taken by the monitor simultaneously with the measurement of the spectrum is shown in Fig. 6, and indicates a half-life of 107±3 min., in adequate agreement with the more accurate half-life of Bleuler *et al.* The spectrum, corrected for counter window absorption, but uncorrected for finite resolution at the high energy tail, is shown in Fig. 7. The Fermi plot is a straight line down to about 160 kev, indicating that the spectrum is of the allowed shape. Correcting for finite resolution on the tail of the spectrum brings those points practically into the straight line. The discrepancy, which does not greatly exceed experimental error, might be due to the very small fraction of high energy betas in the second group. These would not be detectable, because of the very low intensity, except perhaps near the end point of the low energy group. No internal conversion of the γ-ray is found; this is to be expected in view of its high energy. The extrapolated end point from the data uncorrected for source window absorption is 1240 kev; correcting for this absorption (5 kev at high energies) gives 1245±5 kev. This agrees satisfactorily with the value of Bleuler, Boltmann, and Zünti which is 1180±50 kev. The value calculated for ft, using $Z=19$ (residual nucleus), $\epsilon_0=1245$ kev and 109.4 min. for t, is 1.26×10^5 sec., which puts the transition $A^{41}\rightarrow K^{41}+e^-$ into the "allowed" (forbidden only by the difference in symmetry of the nuclear wave functions) class for medium nuclei.

B. Oxygen 15

The O^{15} spectrum was first investigated in a cloud chamber by Fowler, Delsasso, and Lauritsen[14] who found that O^{15} emitted positrons with an end point of 1.7 Mev, using the K−U extrapolation. A recent

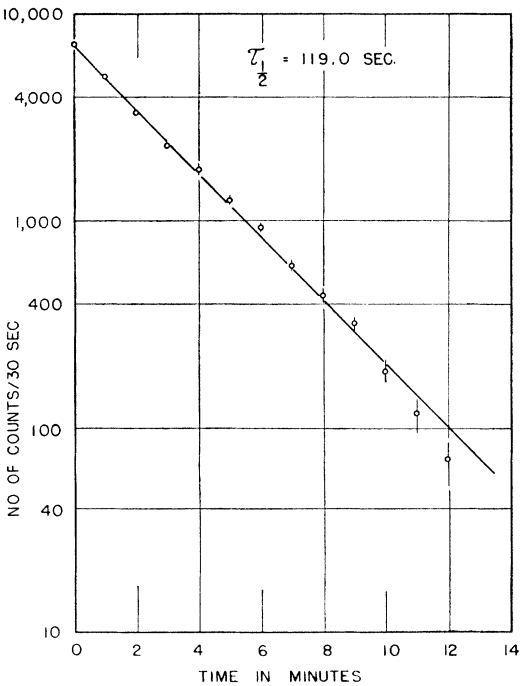

FIG. 8. Decay curve of O^{15}. Each point represents the number of counts over a 30-sec. period, corrected for background and counter deadtime.

[27] Kurie, Richardson, and Paxton, Phys. Rev. **49**, 368 (1936).
[28] Bleuler, Boltmann, and Zünti, Helv. Phys. Acta **19**, 419 (1946); **20**, 195 (1947).

measurement using absorption in aluminum, by Sherr, Meuther, and White,[29] gave an end point of 1.68 Mev.

Using nitrogen gas continuously circulated, O^{15} was produced by the N^{14} (d, n) reaction. The deuteron beam passing through the bombardment chamber was about 20μ amp. For accurate measurement of the half-life a cylindrical disintegration chamber of copper, with a 1-cm hole covered with Cu foil, was substituted for the source chamber. By taking counts over 30-sec. intervals out of every minute, decay curves showing the half-lives were obtained. A sample decay curve, corrected for counter background and deadtime, is shown in Fig. 8. The half-life of O^{15} as obtained from a series of eight decay curves, is 118.0 ± 0.6 sec., which is somewhat lower than previous values.[30] The linearity of the logarithmic plot of the decay curves indicates that only one activity is present, as would be expected on the basis of the isotopic abundance and relative cross sections involved in the competing reactions, the most important of which (N^{14} (d, p)) produces inactive N^{15}.

The spectrum was taken by the method previously described. Figure 9 shows the Fermi plot obtained from it. It gives an end point (corrected for source-window absorption at high energies) of 1.683 ± 0.005 Mev, which agrees with the cloud-chamber and absorption measurement results within their experimental errors. The graph shown is the result of four runs, normalized to the same value in the intermediate energy region (500 to 800 Mev).

The Fermi plot is essentially linear down to an energy of about 300 kev. Some slight curvature away from the axis might be inferred, but its departure from a straight line, if any, is very small and could be attributed to source thickness, which has the effect of giving the observed spectrum a more positive curvature.

Below 300 kev the Fermi plot deviates sharply from linearity, showing an excess of positrons experimentally. This is probably due to the combined effect of source thickness and source window thickness. Since the pressure in the source chamber is 25 cm Hg, the equivalent thickness of the gas is 1 mg/cm^2; the window thickness was about 2.6 mg/cm^2. The effect of source thickness plus the straggling of β-particles in the window could combine to make the O^{15} curve deviate from the theoretical allowed shape at a higher energy than the A^{41}, as is the case. Taking the window thickness plus half the source thickness as an approximate value to compare with the White-Millington data gives 2.3 mg/cm^2 for A^{41} and 3.2 for O^{15}. $\Delta(H\rho)/H\rho$ due to thickness becomes equal to the spectrometer resolution half-width (3 percent) for 160 and 260 kev respectively. These are near the observed points of deviation.

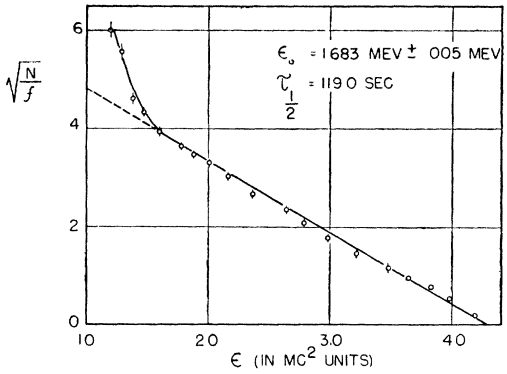

FIG. 9. Fermi plot of the O^{15} β-spectrum (positrons).

The curve for O^{15} thus indicates an allowed spectrum, though the possibility of a compound spectrum is not completely excluded. This is what is expected from such a "mirror image" transition of the Wigner series. The ft value calculated from $\epsilon_0=1.683$ Mev, $t_{\frac{1}{2}}=118.0$ sec. and $Z=7$, is 3910 sec., which is of the same order as the other emitters in group OA (light emitters of the allowed class). The mass difference between O^{15} and N^{15} is $\epsilon_0+2mc^2=2.705$ Mev. Since N^{15} has a measured mass of 15.00489 amu, the mass of O^{15} is 15.00780 amu.

ACKNOWLEDGMENTS

We should like to express our gratitude to Professor W. W. Havens, Jr., who suggested the problem, and to Professors J. R. Dunning, L. J. Rainwater, and E. T. Booth, and Dr. C. S. Wu for their constant advice and encouragement. Thanks are also due to Miss Miriam Levin and the cyclotron crew for their continued willing assistance.

We should also like to thank the United States AEC, which aided materially in the performance of this research.

[29] Sherr, Meuther, and White, Phys. Rev. **75**, 282 (1949).
[30] W. Bothe and W. Gentner, Zeits. f. Physik **112**, 45 (1939).